A. C. Electronic Tunneling at Optical Frequencies

S. M. Faris, B. Fan* and T. K. Gustafson

Department of Electrical Engineering and Computer Sciences
and the Electronics Research Laboratory
University of California, Berkeley, California 94720

ABSTRACT

Rectification characteristics of non-superconducting metal-barrier-metal junctions deduced from electronic tunneling have been observed experimentally for optical frequency irradiation of the junction. The results provide verification of optical frequency Fermi level modulation and electronic tunneling current modulation.

Research sponsored by the National Science Foundation, Grant GK-33939 and by the National Aeronautics and Space Administration, Grant NGR-05-003-559.

*Also of Lawrence Berkeley Laboratory, University of California, Berkeley California 94720

We wish to report evidence of optical frequency rectification with small-area potential barriers located between two normal metallic conductors. Experimental observations are in agreement with semi-classical predictions based upon electronic tunneling induced by an optical frequency modulation of the Fermi levels of the metals on either side of the barrier.

Since the thickness and cross-section area of the barrier are much smaller than the wavelength, the rectification can be described quasi-statically in terms of the current-voltage (I-V) characteristic. An adequate semi-classical treatment assumes a free-electron model and a potential barrier modified from a trapezoidal shape by the influence of surface charges, in part due to the images of the tunneling electrons in the two metals (Fig. 1). The I-V characteristic is then given by[1]

$$I_f(V) = J_f\{\bar{\phi}_f \exp(-A_f \bar{\phi}_f^{1/2}) - (\bar{\phi}_f + eV)\exp[-A_f(\bar{\phi}_f + eV)^{1/2}]\};\ V > 0$$

$$I_r(V) = J_r\{(\bar{\phi}_r - eV)\exp[-A_r(\bar{\phi}_r - eV)^{1/2}] - \bar{\phi}_r \exp(-A_r \bar{\phi}_r^{1/2})\};\ V < 0 \qquad (1)$$

I_f is the forward current and I_r the reverse current where V is positive when the higher work function metal (metal 2) is negative with respect to the other metal (metal 1). The current is of the same sign as the voltage. The definitions of the parameters and the potential barrier profiles are given in Fig. 1: $A_i = [4\pi\Delta s/h](2m^*)^{1/2}$, i = f, r and $\Delta s = s_2 - s_1$ where s_2 and s_1 are the classical turning points given by $\phi_f(x) = 0$ and $\phi_r(y) = 0$ respectively. m* is the effective electronic mass in the metals. $\bar{\phi}_f = \int_{s_1}^{s_2} \phi_f(x)\, dx/\Delta x$ and $\bar{\phi}_r = \int_{s_1}^{s_2}$

$\phi_r(y)\, dy/\Delta s$. These average barrier potentials $\bar{\phi}_f$ and $\bar{\phi}_r$ can be written as $\alpha_i - e\beta_i V$, $i = f, r$ where α_i and β_i vary slowly with voltage and $\beta_i = (s_1 + s_2)/2s$. $J_i = \sigma e/[2\pi h(\Delta s)^2]$, where e is the magnitude of the electronic of the electronic charge, h Planck's constant and σ the contact area.

The significant features of the experimental results to be discussed are well explained by assuming that the most important consequence of the radiation field is the potential drop across the barrier between the two metals.[2] Thus

$$V(t) = V_b + v(t)\cos \omega t \tag{2}$$

where V_b is the bias voltage and v(t) is the envelop of the induced voltage at frequency $\omega/2\pi$ of the irradiating field. Substituting Eq. (2) into Eq. (1), and then averaging the tunneling current over a period of the optical oscillation gives the rectified current:

$$I_{rect}(t) = \int_{-\pi}^{\pi} I(V_b + v(t)\cos\theta)\, d\theta/2\pi \tag{3}$$

where $\theta = \omega t$ and v(t) is assumed to be slowly varying over one optical cycle. It is understood that $I = I_f$ when its argument is positive and $I = I_r$ otherwise.

Numerical calculations have been performed assuming the optical voltage envelop v(t) to be a square wave with a period $2\pi/\Omega$. For the rectified component at $\Omega/2\pi$, plotted as a function of the bias voltage in Fig. 2, the optical voltage amplitude is sufficiently small for the

signal V_Ω to be directly proportional to the second derivative d^2I/dV^2 evaluated at the bias point of the I-V characteristic taken at frequency $\omega/2\pi$.[3] For any thickness of the barrier $d^2I/dV^2 < 0$ at $V_b = 0$ so that V_Ω for zero bias is predicted to be negative.

The striking evolution of the V_Ω-V_b profiles with increasing barrier thickness displays curvature in the I-V characteristic which is a direct consequence of the optical Fermi modulation and the basic tunneling model as represented by Eq. (1).

For thin barriers ($s < 7\text{Å}$), the $V_\Omega - V_b$ profile is, to a good approximation, a straight line with negative slope (curve I). Thus the I-V characteristic has a negative curvature for positive bias and positive curvature for negative bias. Since for this range the linear conductance is large and dominates, this curvature change is not apparent in the I-V characteristic which is linear to within a percent or less. As the barrier thickness is increased to an intermediate range ($7\text{Å} \leq s < 7.5\text{Å}$) although the linear conductance still dominates the I-V characteristic, the $V_\Omega - V_b$ profile and hence the curvature in the I-V characteristic evolves to an " "-shape (curve III). This behavior indicates a complicated I-V characteristic in which the curvature changes four times as V_b is varied from a large negative value to a large positive value.

As s is increased further ($7.5\text{Å} \leq s < 12\text{Å}$), an exponential increase in V_Ω with increasing V_b occurs in the " "-shaped profile near $V_b = 0$ (curve IV). It is noted in addition that the two biases V_b^+ and V_b^- at which V_Ω changes sign increase in absolute value as s is increased.

Finally for s large ($s \geq 12\text{Å}$), the most familiar and expected behavior is predicted, that of an exponentially increasing V_Ω displaying the essential features of Eq. (1) for a relatively large value of A

(curve V). This experimentally corresponds to the transition or field emission region.[4] The linear conductance no longer dominates and the exponential dependence is readily apparent in the I-V characteristic.

The evolution in the $V_\Omega - V_b$ profile with barrier thickness can be reasonably described with an analytical expression for $I_{rect}(t)$ obtained by expanding the square roots in the exponentials of Eq. (1). Keeping only the terms linear in v(t) and defining a parameter $z_i = \beta_{ib} A_{ib} (4\bar{\phi}_{ib})^{-1/2}$, one obtains

$$I_{rect}(t) \simeq J_i \exp(-A_{ib}\bar{\phi}_{ib}^{1/2})\{\bar{\phi}_{ib}[I_o(z_i v) - 1] - \beta_{ib} v I_1(z_i v)$$

$$-J_i \exp(-A_{ib}\bar{\phi}_{ib}^{1/2})\{\bar{\phi}_{ib}[I_0(z_i' v) - 1] - \beta_{ib} v I_1(z_i' v)\} \quad (4)$$

The subscript b indicates evaluation of the parameters at the bias V_b; i = f when $V_b \geq 0$ and i = r when $V_b \leq 0$. The primed parameters are identical but with β_{ib} replaced by $1 - \beta_{ib}$. I_0 and I_1 are the modified Bessel functions of zeroth and first order, respectively. Further expansion of Eq. (4) in terms of v and V_b gives the expansions discussed earlier[5] for thin barriers.

Detection experiments using an arrangement similar to that described in Ref. 5 have verified the detailed $V_\Omega - V_b$ evolution deduced above. In the experiments, a 6-mW, 6328-Å He-Ne laser beam was chopped at 886Hz and focused onto metal-metal point contact junction (tungsten whisker on a gold post). The phase-sensitively detected voltage signal at 886Hz, plotted as a function of bias, is shown in Fig. 3. Various junction resistances are achieved by varying the contact

pressure (a large junction resistance corresponds to a large barrier thickness).

The measured signal is negative at $V_b = 0$ for all junction resistances agreeing with the theoretical prediction. One also observes linear $V_\Omega - V_b$ profile with negative slope for a small junction resistance ($\lesssim 2\Omega$). For large junction resistance ($\gtrsim 5M\Omega$) the profiles are exponential with a positive slope.[6] The intermediate regime in which a transition from one to the other occurs is also evident and displays the detailed evolution predicted theoretically. The exponential increase in V_Ω with V_b for small V_b is apparent in many of the profiles which display a turning-over of the signal with a large bias voltage.

These experimental results verify the predictions of optically modulated electronic tunneling theory for the metal-barrier-metal junction behavior. The characteristic experimental evolution of the $V_\Omega - V_b$ profiles for changing resistance is a direct consequence of optical rectification and, in particular, of the variation of the tunneling parameter $\gamma = A\alpha^{1/2}$. Hence the evolution of the $V_\Omega - V_b$ is predicted over some range of s for <u>any</u> set of values of the various junction parameters such as ϕ_1, ϕ_2, ε, m^*.

The junction, on the basis of the present results, mixing experiments[7], and re-radiation experiments[8] demonstrates a microscopic time response which is at least as short as the inverse of the visible frequencies. The upper limit of this time response is expected to be the time taken for the electrons to tunnel through the barrier between the two metals which has been shown to be as short as 10^{-16}s[9].

REFERENCES

1. J. G. Simmons, J. Appl. Phys., 34, 2581 (1963).
2. In particular, we are neglecting the mixed character of the electronic states due to elementary excitations induced by the fields. Such photon-induced effects are expected to be important but should not influence the general rectification characteristics discussed here.
3. For increased optical intensities, other nonlinear optical effects such as signal polarity reversal are predicted. An approximate analysis and initial experimental observations for thin barriers are reported in Ref. 5.
4. R. Young, J. Ward, and F. Scire, Phys. Rev. Lett., 27, 922 (1971).
5. S. M. Faris, T. K. Gustafson, and J. C. Wiesner, IEEE J. Quantum Electron., QE-9, 737 (1973).
6. This is the region which is applicable for the metal-barrier-metal structures produced thus far: J. G. Small et al., Appl. Phys. Lett., 24, 275 (1974); T. K. Gustafson, et al., Appl. Phys. Lett., 24, 620 (1974).
7. E. Sakuma and K. M. Evenson, IEEE J. Quantum Electron., QE-10, 599 (1974). Recently these mixing experiments have also been shown to be in accord with quasi-static tunneling theory (S. M. Faris and T. K. Gustafson, Appl. Phys. Lett., 25, Nov. 1974). For these experiments, in contrast to the optical experiments, the current is found to be the independent variable. Thus the signal-bias dependence displays current derivatives of the voltage as a function of the bias current rather than voltage derivative of the current. Presumably the difference results from the associated antenna

structure, which is either absent or lossy at optical frequencies for structures considered thus far.

8. A. Sanchez, S. K. Singh, and A. Javan, Appl. Phys. Lett., 21, 240(1972).

9. T. E. Hartman, J. Appl. Phys., 33, 3427 (1962). It should be pointed out that the RC time constant of the device is not related to the microscopic speed of response but to the coupling of the junction to the radiation field. If C is the junction capacitance, then for frequencies for which $R >> (\omega C)^{-1}$ high reflectivity of the incident power due to re-radiation is expected unless the junction is matched properly to the radiation field. Reciprocally, the rapid microscopic response of the junction can only be displayed externally if the junction and coupling device together have an appropriately small RC time constant in addition to the short microscopic time response.

FIGURE CAPTIONS

Fig. 1. Simplified energy band diagram for a metal-barrier-metal structure. E_{F_1} is the Fermi energy of metal 1 and E_{F_2} is the Fermi energy of metal 2. ϕ_1 and ϕ_2 are the work functions of the two metals. S is the barrier thickness. The effective potential taken with respect to E_{F_2} for a forward based junction (metal 2 negative with respect to metal 1) is $\phi_f(x) = \phi_2 - (\Delta\phi + ev)x/s - \lambda s^2/x(s-x)$. Where $\Delta\phi = \phi_2 - \phi_1$ λ, which specifies the amount of induced surface charge is equal to $1.15\ e^2\ \ell n\ 2/8\pi\varepsilon s$ for plane parallel geometry and charge induced by the tunneling electrons (image charge). ε is the dielectric constant of the barrier. For a reverse bias the effective potential with respect to E_{F_1} is $\phi_r(y) = \phi_1 + (\Delta\phi + ev)\ y/s - \lambda s^2/y(s-y)$ where $y = s-x$.

Fig. 2a. Theoretical calculations of the I_Ω-V_b characteristics using Eq. (3) for the short circuit current and the circuit diagram shown for the equivalent circuit of the detection electronics. $G_T = \left.\frac{dI}{dV}\right|_{V_b}$ from Eq. (1) G_b is the shunt conductance associated with the bias circuit and G_L is the combined load resistance of the lockin amplifier, and X-Y recorder equal to $2\times10^{-6}\Omega^{-1}$. The device area $S = 10^{-10}cm^2$, the optical voltage $v = .15V$, $\phi_1 = 4.38eV$, $\phi_2 = 4.46$, $\Delta\phi = 0.08$. Curves I-III have respectively barrier thickness, 5 of 6.9, 7.1 and 8.4Å $G_T >> G_L + G_b = 1.2\times10^{-6}\Omega^{-1}$. For curve IV s = 8.75Å and $G_T \sim G_b = 5\times10^{-4}\Omega^{-1}$. For curve V s = 16Å and $G_T << G_L + G_b = 1.2\times10^{-6}\Omega^{-1}$.

Fig. 2b. Experimentally measured V_Ω-V_b characteristics as obtained from tungsten whisker on platinum point contact diodes of varying tunneling conductances. The detection electronics of Fig. 2a is applicable. The zero bias junction conductances G_T for curves I-IV are $.5\Omega^{-1}$, $10^{-2}\Omega^{-1}$, $2\times10^{-3}\Omega^{-1}$ and $5\times10^{-3}\Omega^{-1}$ respectively. For curve V $G_T\Big|_{V_b=0} = 10^{-7}\Omega^{-1}$ making $G_B + G_L$ dominant.

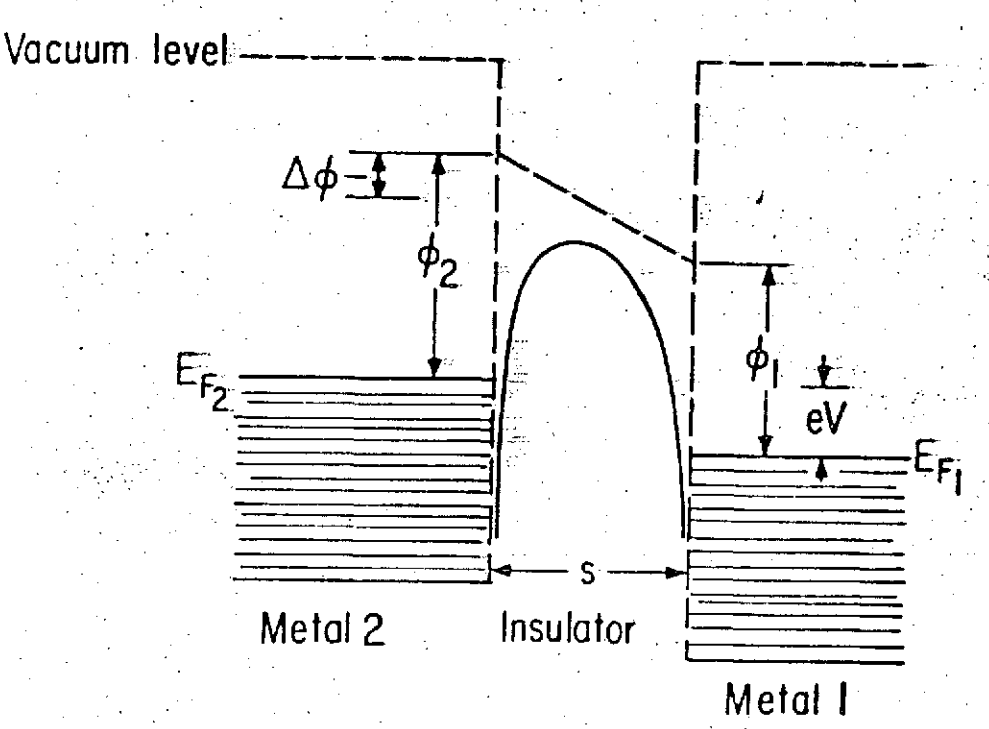

POTENTIAL BARRIER OF M-B-M JUNCTION

Fig. 1

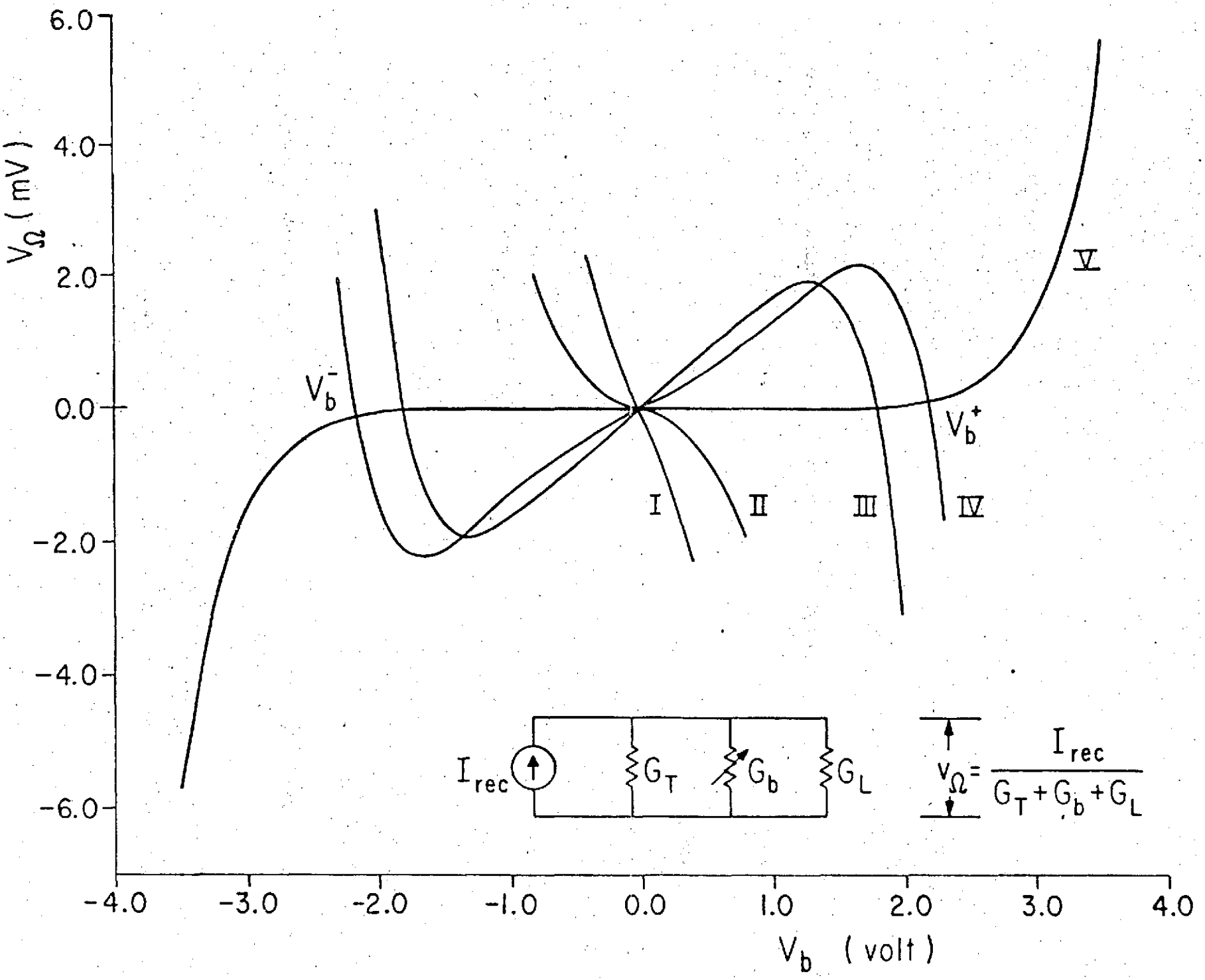
6.0
4.0
2.0
0.0
-2.0
-4.0
-6.0
V_Ω (mV)
V_b^-
V_b^+
I
II
III
IV
V
I_{rec}
G_T
G_b
G_L
$V_\Omega = \frac{I_{rec}}{G_T + G_b + G_L}$
-4.0
-3.0
-2.0
-1.0
0.0
1.0
2.0
3.0
4.0
V_b (volt)

Fig. 2a

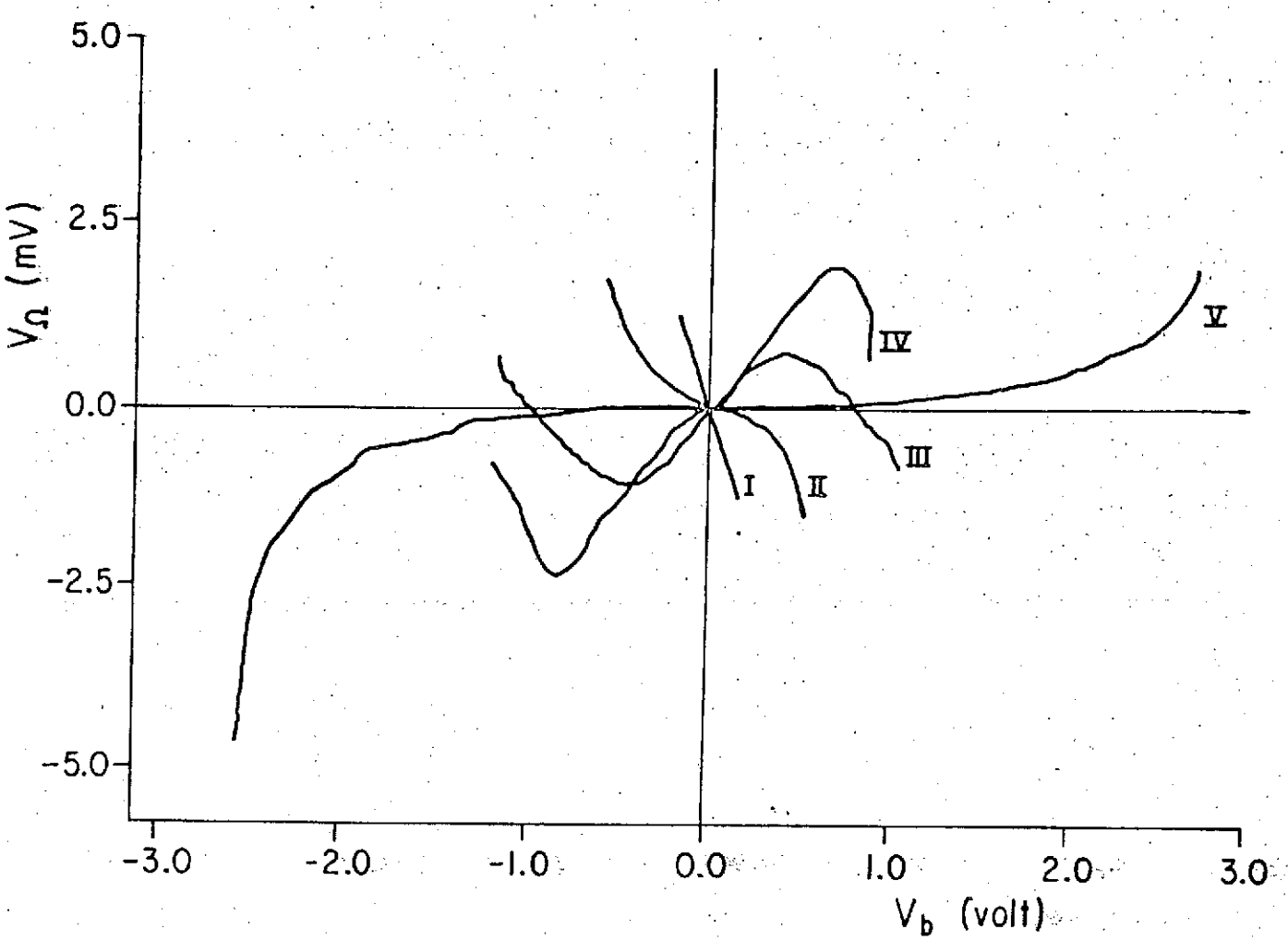

Fig. 2b